Structure−Property Correlations of Atomistic and Coarse-Grained Models of Polymer Melts

K. S. Schweizer,* E. F. David, and C. Singh

Departments of Materials Science & Engineering, Chemistry and Materials Research Laboratory, University of Illinois, 1304 West Green Street, Urbana, Illinois 61801

J. G. Curro

Sandia National Laboratories, Albuquerque, New Mexico 87185

J. J. Rajasekaran

Advanced Materials Laboratory, University of New Mexico, Albuquerque, New Mexico 87106

Received September 23, 1994; Revised Manuscript Received December 3, 1994®

ABSTRACT: Polymer reference interaction site model (PRISM) integral equation theory of polymer melts is applied to investigate the role of local chemical structure on interchain packing and thermodynamic properties such as the isothermal compressibility, cohesive energy, and solubility parameters. Chemically realistic rotational isomeric state model (RIS) level calculations are carried out for polyethylene and isotactic and syndiotactic polypropylene. A strong correlation between the thermodynamic properties and the local depletion regime of interchain packing is found. A series of coarse-grained models of decreasing local realism are then investigated, and various schemes are constructed to estimate the coarse-grained model parameters in terms of polymer structure. For the discrete semiflexible chain and the Gaussian thread models the effects of backbone characteristic ratio and chain branching are incorporated by employing an effective stiffness, or aspect ratio. A strategy for carrying out the mapping from the atomistic to coarse-grained level based on single-chain conformational and interchain packing considerations is studied. For polyethylene and polypropylene, by enforcing an equality of the zero-angle scattering of the atomistic and coarse-grained models, good agreement is found between the local radial distribution functions and reduced solubility parameters predicted by the various models. Numerical predictions of the semiflexible chain model and analytical results for the Gaussian thread liquid are obtained and compared against RIS-level calculations and experimental estimates of the melt solubility parameters. At least within a homologous series of materials, it appears that appropriately calibrated coarse-grained descriptions can reproduce various structural and thermodynamic properties. This suggests that polymer alloy miscibility can be studied within a homologous series of materials by computationally convenient, coarse-grained models.

I. Introduction

The connection between polymer chemical structure and bulk phenomena is of great practical importance in materials science and engineering, and a subtle fundamental problem in statistical mechanics. Traditional theoretical approaches have employed chemically unrealistic, heavily "coarse-grained" models and/or a fictitous lattice representation of continuous space. Recently, new approaches based on modern polyatomic liquid state theory have been developed which are known collectively as the "polymer reference interaction site model" (PRISM) theory.[1,2] This microscopic theory allows a continuous space, chemically realistic description of polymer liquids and their phase transitions. The question of how chemical structural features on different length scales influence interchain packing and bulk thermodynamic behavior can be systematically studied. In particular, we would like to understand what aspects of molecular structure are really essential for understanding a particular property or phenomenon. In this paper we explore the possibility of constructing relatively simple coarse-grained homopolymer models in a manner which reproduces observable bulk properties of fluids of complex, often branched, one-component polymer melts.

The physical properties of present interest include the isothermal compressibility, cohesive energy density, solubility parameter, and interchain pair correlation function. Besides the obvious relevance of these quantities to equilibrium melt questions such as the equation of state, we intend to investigate how an understanding of structure−property correlations in melts might be used to make predictions about polymer alloy miscibility. Recent experimental work on polyolefin melts and blends[3−7] has re-emphasized the long-held belief that the one-component liquid properties exert a profound influence on the phase behavior of polymer mixtures.[8,9] This aspect will be studied in depth in future publications.

The general philosophy of this work is sketched in Figure 1. Using PRISM theory we first study the structure and thermodynamic properties of atomistic rotational isomeric state (RIS) models[10] of hydrocarbon polymer liquids. This model is then subjected to an intermediate level of coarse-graining where several local chemical features are still retained. For example, in the semiflexible chain (SFC) model[11,12] the macromolecule is characterized by three local length scales: the effective monomer diameter, an effective bond length which controls the accessible surface area of a monomer, and a bending energy which imparts local rigidity to the polymer and controls the chain persistence length or aspect ratio. The most coarse-grained model is the Gaussian thread chain, which is infinitely thin and flexible on all length scales. This model is locally characterized only by the statistical segment length and is generally adopted in field theoretic studies. Within PRISM theory it has the technical advantage that

* To whom correspondence should be sent.

® Abstract published in *Advance ACS Abstracts,* February 1, 1995.

0024-9297/95/2228-1528$09.00/0

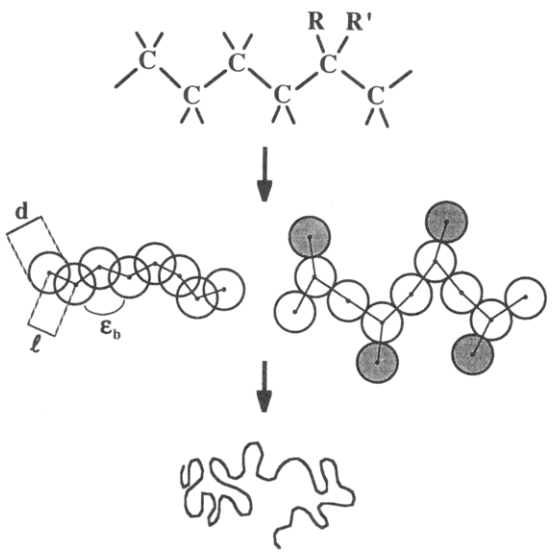

Figure 1. Schematic representation of the coarse-graining procedure and the three levels of models considered: (i) an atomistic RIS level, (ii) two intermediate-level models, and (iii) the Gaussian thread. In the overlapping semiflexible chain (SFC) model, the parameter ϵ_b is a bending energy which controls the persistence length of the polymer.

analytical results can often be derived which provide considerable insight.[12-18]

A fundamental question of interest is whether one can develop a scheme to choose the parameters of a particular coarse-grained model to reproduce selected bulk interchain properties of the chemically realistic model. We shall refer to such an operation as a "mapping" or "calibration" procedure. Unfortunately, a rigorous renormalization-group-like scheme for accomplishing this does not exist, and thus physically motivated, but heuristic, procedures must be employed. Our existing theoretical understanding at the atomistic level is by far most complete for the structurally simplest polymer, polyethylene. PRISM theory has been employed to treat the interchain correlations,[19-21] scattering structure factor,[19,20] equation of state, and other thermodynamic properties[22,23] of an RIS-level description of polyethylene melts. Moreover, spatially inhomogeneous situations have also been treated: density functional[24,25] and wall-PRISM[22,26,27] theory for the structure of polyethylene and *n*-alkanes near a surface and in confined spaces, and polymer density functional theory to treat polyethylene crystallization from the melt.[28] Good agreement of these *ab initio* studies with experiment and/or simulation has been documented. Thus, polyethylene is the first case considered and will represent the benchmark system for carrying out the mapping procedure and calibration process. Although we believe our ideas are of general utility, applications in this paper focus on polyolefins due to the simplicity of chemical interactions in saturated hydrocarbon systems and our interest in treating hydrocarbon alloys using coarse-grained models.

The remainder of the paper is organized as follows. In section II we briefly summarize PRISM theory and the properties of interest. Selected numerical predictions for RIS models of polyethylene and polypropylene melts are presented, and comparisons to experimental data are made. Intermediate-level models are studied numerically in section III, and the question of how to map real structures onto such models is addressed. Analytical results for the Gaussian thread model are derived in section IV and compared against the behavior of atomistic models, experiments, and the predictions of some prior theories. A summary and brief discussion of the application of our results to polymer alloy miscibility is presented in section V.

II. PRISM Theory, Atomistic Models, and Effective Aspect Ratios

RIS models contain angstrom-level information about molecular structure, e.g., bond lengths, bond angles, torsional potentials, etc. Although much work has been done at the single-chain level, atomistic simulations of chemically realistic polymer melts are rare due to the great computational demands. However, much effort has been recently spent on simulating alkane fluids, so reasonably accurate intra- and intermolecular potential models are available for simple hydrocarbons.[29] In this section we employ standard RIS models of polyethylene and polypropylene using well-documented computational procedures.

A. Models and PRISM Theory. For atomistic models we employ a Lennard-Jones potential between spherically symmetric carbon centers given by

$$u(r) = 4\epsilon_{LJ}\left[\left(\frac{\sigma_{LJ}}{r}\right)^{12} - \left(\frac{\sigma_{LJ}}{r}\right)^{6}\right] \qquad (2.1)$$

where we have used the common united-atom description which collapses the hydrogens onto the carbon center. At melt densities in a one-component fluid, the van der Waals idea that the intermolecular *structure* of a dense liquid is dominated by the repulsive forces applies.[30-32] We employ this philosophy for the calculation of intermolecular pair correlations. In numerical implementation of PRISM a hard core potential with a temperature-dependent site diameter $d(T)$ is used to mimic the repulsive branch of the potential according to the standard Barker–Henderson procedure.[23,33] Computations based on the continuous repulsive Lennard-Jones potential can be done. However, for our present illustrative purposes, and the desire to compare atomistic and coarse-grained models, an effectively hard core potential model is most appropriate.

Calculation of structural quantities employs the PRISM theory which consists of the generalized matrix Ornstein–Zernike equation(s) in Fourier space:[1,32,34]

$$\hat{\mathbf{h}}(k) = \hat{\omega}(k)\,\hat{\mathbf{C}}(k)[\hat{\omega}(k) + \varrho\hat{\mathbf{h}}(k)] \qquad (2.2)$$

plus the Percus–Yevick closure for hard core potentials:

$$g_{\alpha\gamma}(r) = 0, \quad r < \mathrm{d}_{\alpha\gamma}$$

$$C_{\alpha\gamma}(r) = 0, \quad r > d_{\alpha\gamma} \qquad (2.3)$$

Here, ϱ_α is the number density of sites of type α, $\hat{\omega}(k)$ is the single-chain structure factor matrix, $\hat{\mathbf{C}}(k)$ is the matrix of site–site direct correlation functions, and $\hat{\mathbf{h}}(k)$ is the matrix of site–site intermolecular total correlation functions. The corresponding radial distribution functions are $g_{\alpha\gamma}(r) = h_{\alpha\gamma}(r) + 1$. Neglecting end effects in the usual manner,[34,35] there is one nonlinear integral equation for polyethylene and six coupled equations for polypropylene (three symmetry-inequivalent sites). These integral equations are solved using the Picard iteration method.[31] The matrix of collective scattering structure factors is given by

$$\hat{\mathbf{S}}(k) = \hat{\omega}(k) + \varrho\hat{\mathbf{h}}(k) = (1 - \hat{\omega}(k)\,\varrho\hat{\mathbf{C}}(k))^{-1}\hat{\omega}(k) \qquad (2.4)$$

For polyethylene, or any single-site homopolymer model, the $k = 0$ value of the structure factor is simply related to the isothermal compressibility, κ_T, by the thermodynamic identity

$$\hat{S}(0) = \varrho k_B T \kappa_T \tag{2.5}$$

where ϱ is the total site number density.

We shall also be interested in the cohesive energy density, defined as

$$U \equiv \frac{1}{2}\sum_{\alpha,\gamma} \varrho_\alpha \varrho_\gamma \int d\vec{r}\; V_{\alpha\gamma}(r)\, g_{\alpha\gamma}(r) \tag{2.6}$$

where $V_{\alpha\gamma}(r)$ is the attractive branch of the carbon–carbon interaction potential between sites α and γ. The standard thermodynamic perturbation approach is employed, i.e., the "high-temperature approximation" (HTA), corresponding to evaluating the interchain pair correlations from the *purely repulsive* force (hard core) reference fluid.[31,32]

$$g_{\alpha\gamma}(r) \cong g^{(0)}_{\alpha\gamma}(r), \qquad \text{HTA}$$
$$\equiv g_0(r) \text{ for single-site model}$$

The precise form of the attractive potential employed will vary depending on what level of single-chain model is employed. For the RIS model we again follow the Barker–Henderson scheme[33] where:

$$V(r) = 4\epsilon_{LJ}\left[\left(\frac{\sigma_{LJ}}{r}\right)^{12} - \left(\frac{\sigma_{LJ}}{r}\right)^{6}\right], \qquad r > \sigma_{LJ}$$
$$= 0, \qquad r < \sigma_{LJ} \tag{2.7}$$

The Lennard-Jones energy and length parameters for methylene units have been estimated by many workers and fall in the range of $\epsilon_{LJ} = 40$–60 K and $\sigma_{LJ} = 3.9$–4.4 Å, respectively. In our present calculations we follow the recent PRISM work on alkanes and polyethylene where the appropriate parameters are[19,23,28] $d = 3.9$ Å and $T = 430$ K, $\epsilon_{LJ} = 40$ K, and $\sigma_{LJ} = 4.35$ Å. Interestingly, this methylene group diameter value is in excellent accord with a simple estimate based on the methylene number density $\varrho = 0.0334/\text{Å}^3$ at $T = 430$ K: $d = (6 \times (\text{site volume})/\pi)^{1/3} = (6/\varrho\pi)^{1/3} \cong 3.87$ Å.

B. Solubility Parameters and Effective Aspect Ratios. The solubility parameter, δ, is defined in the standard manner as[36]

$$\delta \equiv (-U)^{1/2} \tag{2.8}$$

This simple formula is actually quite subtle in the sense that information concerning the bare chemical interaction potentials and chain structure and packing enter in a *nonseparable* manner which will have important thermodynamic consequences. A reduced solubility parameter, $\tilde{\delta}$, defined as the ratio of δ to its value in a hypothetical random continuum fluid, i.e., $g_{\alpha\gamma}(r) = 1$ for $r > d_{\alpha\gamma}$, is defined as

$$\tilde{\delta} \equiv \left(\frac{\sum_{\alpha,\gamma} \varrho_\alpha \varrho_\gamma \int d\vec{r}\; V_{\alpha\gamma}(r)\, g_{\alpha\gamma}(r)}{\sum_{\alpha,\gamma} \varrho_\alpha \varrho_\gamma \int d\vec{r}\; V_{\alpha\gamma}(r)}\right)^{1/2} \tag{2.9}$$

Since the interchain attractive potentials are very short range, the value of this quantity is a direct reflection of the deviation of intermolecular contact probability from its random value. Note that the solubility parameter is dominated by the local packing in the fluid, i.e., structure on the length scale of the attractive potential range. For high polymers the long-range intermolecular structure enters only as a weak finite size correction to the local pair correlation function.

For both atomistic RIS models and more coarse-grained descriptions we shall be interested in characterizing an effective stiffness of the chain in a manner that reflects the polymer's interchain packing ability. A useful quantity for this purpose is an "aspect ratio". A "bond-level" definition, which is particularly appropriate for an unbranched RIS chain such as polyethylene, is given by

$$\Gamma_{bond} \equiv \frac{(6R_g^2/N_b)^{1/2}}{d} \equiv \frac{\sigma_{bond}}{d} \tag{2.10}$$

where R_g is the radius of gyration, N_b is the number of *backbone bonds*, and σ_{bond} is an effective statistical segment length. The subscript "bond" refers to the fact that the above definition is on a single-bond, or methylene group, basis. A "bond-level" definition appropriate for polyolefins of identical chemical formula but different microstructures and degrees of branching is given in terms of the polyethylene value as

$$\Gamma_{bond} \equiv \Gamma_{bond,PE}\, f_B^{1/3} \left(\frac{C_\infty}{C_{\infty,PE}}\right)^{1/2} \tag{2.11}$$

where f_B is the volume fraction of the monomer contained in the backbone. For a random coil polymer these aspect ratios are not invariant to redefinition of a reference volume. If one employs a reference volume composed of n consecutive methylene groups, then the above numbers would all increase by a factor of $n^{1/6}$.

Since the definition of an aspect ratio is not unique, we shall consider several physically plausible alternatives. A "monomer-level" definition is

$$\Gamma_{mon} \equiv \sigma_{mon}/d_{mon}$$
$$\sigma_{mon} \equiv \left(\frac{6R_g^2}{N_{mon}}\right)^{1/2} = (n_b C_\infty)^{1/2} L \tag{2.12}$$
$$d_{mon} \equiv \left(\frac{6V_{mon}}{\pi}\right)^{1/3} \cong \left(\frac{6}{\pi\varrho_{mon}}\right)^{1/3}$$

where N_{mon} is the number of monomer (repeat units), n_b is the number of backbone bonds per monomer, L is an average backbone bond length, and V_{mon} is the monomer volume estimated as the inverse of the monomer number density. Since monomer volume is highly variable depending on chain structure, a common approach is to introduce an "equal-volume" definition in terms of an (arbitrary) reference volume V_{ref}:

$$\sigma_{ref} \equiv \left(\frac{6R_g^2}{N_{mon}}\frac{V_{ref}}{V_{mon}}\right)^{1/2}, \qquad d_{ref} \equiv \left(\frac{6V_{ref}}{\pi}\right)^{1/3}$$
$$\Gamma_{ref} \equiv \frac{\sigma_{ref}}{d_{ref}} = \Gamma_{mon}\left(\frac{V_{ref}}{V_{mon}}\right)^{1/6} \tag{2.13}$$

When using unbranched, coarse-grained models to

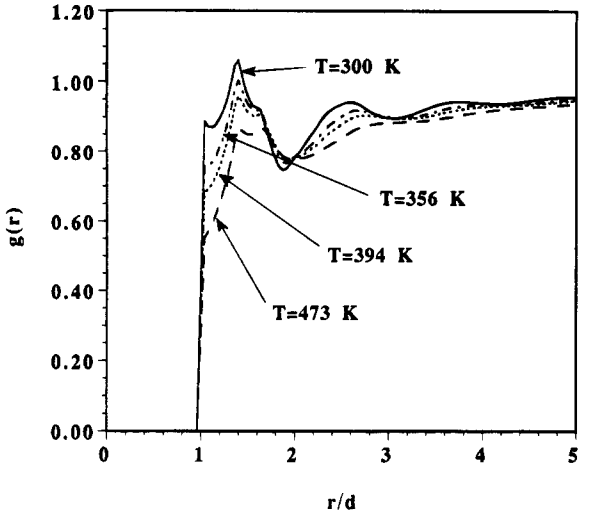

Figure 2. PRISM calculations for the interchain carbon–carbon radial distribution function for an $N = 1000$ RIS model, hard core polyethylene melt. Results are shown for various temperatures as a function of site separation, r, in reduced units of the (temperature-dependent) hard core diameter.

mimic real branched molecules, we feel this definition is probably the most appropriate.

C. Polyethylene Melt. We employ a single-chain RIS structure factor for polyethylene (PE) which is identical to that previously discussed by Honnell et al.[19] and McCoy et al.[37] The characteristic ratio at 300 K is $C_\infty \cong 7.9$. For polyethylene the "bond-level" aspect ratio of eq 2.10 varies as 1.091 ($T = 300$ K), 1.061 ($T = 356$ K), 1.042 ($T = 394$ K), and 1.006 ($T = 473$ K). Although $d(T)$ decreases weakly with increasing temperature,[23] the chain persistence length decreases more rapidly, resulting in the above behavior.

The PRISM calculations for PE melt were carried out exactly as described previously[19] using the experimental number densities as input. Results for the interchain carbon–carbon radial distribution function are shown in Figure 2 for a range of temperatures and $N = 1000$ methylene sites. The most important feature for thermodynamic properties is the presence of a local "correlation hole", i.e., $g(r) < 1$, which deepens as the liquid is heated due to the combined effects of decreasing density and chain persistence length ("stiffness"). This *nonuniversal* local hole is a kind of destructive interference effect which arises from the combined influences of many local chemical length scales and bonding constraints and thermal conformational disorder. Also present is the long-range "universal correlation hole" which arises solely from global chain connectivity and near incompressibility on large length scales.[13,57]

Predictions for the temperature-dependent zero-angle scattering (see eq 2.5) of the repulsive force polyethylene melt are shown in Figure 3. Recall that temperature enters via the intrachain structure factor, the density, and the effective hard core diameter $d(T)$. Comparison with the experiments[38] shows the theory accurately reproduces the magnitude and shape of the data. However, quantitative agreement should not be expected since the contribution of attractive interactions has not been taken into account (although recent arguments by McCoy[39] strongly suggest these are at the 10–20% level in dense melts).

The cohesive energy normalized by its "mean field" Flory value corresponding to $g(r) = 1$ is shown in Figure 4. The normalized cohesive energy is less than unity due to the local correlation hole effect and monotonically

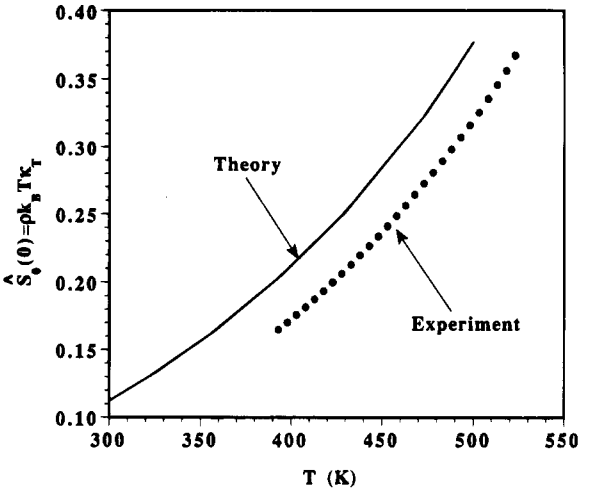

Figure 3. Repulsive force component of the zero-angle collective scattering amplitude for the hard core polyethylene model of Figure 2. Experimental data are from ref 38.

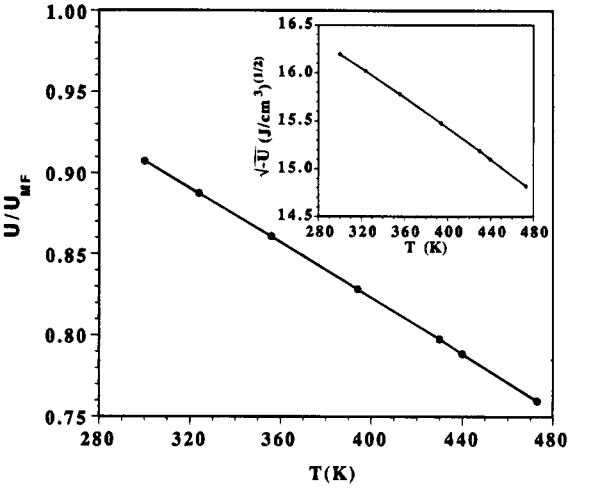

Figure 4. Calculated cohesive energy normalized to its mean field value ($g(r) = 1$) for the hard core polyethylene melt model of Figure 2. The points are the theoretical results and the line is a guide to the eye. Absolute values of the cohesive energy density are shown in the inset.

decreases in roughly a linear manner with increasing temperature. The inset of Figure 4 shows the solubility parameter. The predicted value of 15–16 $(J/cm^3)^{1/2}$ is in excellent agreement with *indirect* experimental estimations based on fitting *PVT* data[6,40] or group molar attraction calculations[41] which yield numbers in the range of 15–19 $(J/cm^3)^{1/2}$. Moreover, even within the thermodynamic perturbative framework (HTA), the magnitude of the slope and roughly linear decrease of the solubility parameter with temperature are in good accord with recent experimental *estimates* of the temperature dependence of polyolefin melt solubility parameters.[3,5,7]

Summarizing, in agreement with the conclusions of prior studies,[19–23,28] it appears that PRISM theory can nearly quantitatively account for the structural and thermodynamic properties of polyethylene melts. This point is significant both for our future studies of polyolefins alloys and also for the mapping and calibration scheme for coarse-grained models we develop in the present paper.

D. Polypropylene Melts. The RIS model of Suter and Flory[42] has been employed to compute the single-chain structure factor of a 400 backbone carbon isotactic polypropylene (i-PP) chain at 473 K. However, the

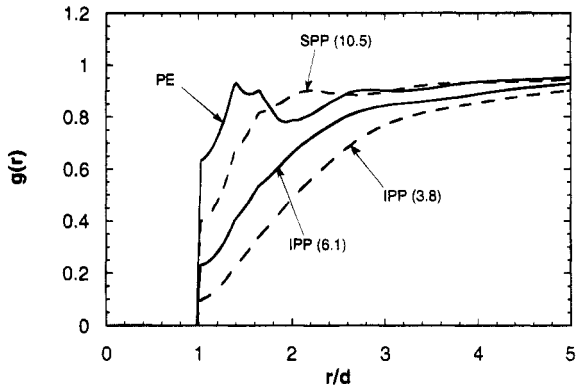

Figure 5. Chain-averaged carbon–carbon intermolecular radial distribution functions at 473 K for an $N_b = 400$ RIS model of hard core polyethylene, isotactic polypropylene, and syndiotactic polypropylene melts. The characteristic ratio of the RIS model employed is shown in parenthesis for polypropylene.

adequacy of this and other RIS models to quantitatively describe i-PP at high temperatures remains unsettled.[43] Hence, the temperature employed in the RIS calculation has been adjusted to reproduce the apparently T-independent experimental value[43] of $C_\infty \cong 6.1$. Many RIS models, including the Suter–Flory one, predict a much smaller characteristic ratio at 473 K. The Suter–Flory model yields $C_\infty \cong 3.8$.

PRISM predictions for the chain-averaged carbon–carbon radial distribution function, $g(r)$, of hard core i-PP at 473 K are shown in Figure 5. Our model of PP consists of three distinct sites which we take as hard spheres of equal $d = 3.9$ Å. As discussed elsewhere,[44] site–site correlations between methyl (CH_3), methylene (CH_2), and methyne (CH) units are not the same due to their different spatial positions in the polymer. The chain-averaged $g(r)$ is computed by averaging over the six symmetry-inequivalent site–site pair correlations. For comparison, results for an $N = 400$ RIS polyethylene melt at the same temperature are also shown. Note that the local correlation hole in i-PP is much deeper, a feature in accord with molecular dynamics simulations.[45] This result can be interpreted in terms of two distinct physical factors: (i) "packing frustration" associated with the presence of the methyl side group which introduces additional chemical length scales and irregularity in monomer shape and (ii) the backbone stiffness of i-PP is smaller than that of PE ($C_\infty \cong 6.6$ at 473 K).

With regards to constructing a coarse-grained model of i-PP, it seems that i-PP "acts on average" as if it was a PE-like molecule but with a much smaller persistence length or aspect ratio. Using eq 2.13 on an equal-volume three-carbon basis (the minimum repeat unit for i-PP), the aspect ratio of PE is 1.21 while that of i-PP is 0.94. The corresponding values on a monomer basis (eq 2.12) are 1.13 and 0.94, and on a bond basis are 1.0 and 0.83, respectively. The usefulness of treating branching in terms of an effective stiffness will be discussed in the next section.

The reduced solubility parameters have been computed using eq 2.9, that Lennard-Jones potential of eq 2.7, and the simplifying assumption that the attractive interactions between all units in i-PP are the same as in PE. The results at 473 K are $\tilde{\delta} = 0.73$ (i-PP) and 0.92 (PE). Thus, i-PP is predicted to have a significantly smaller solubility parameter than PE, i.e., $\delta_{PE}/\delta_{i\text{-}PP} \cong 1.26$.

For comparison, we also show in Figure 5 the PRISM prediction for i-PP using the literal Suter–Flory model at 473 K corresponding to a characteristic ratio of 3.8. As expected, the corresponding local correlation hole in $g(r)$ is even deeper, $\Gamma_{ref} \cong 0.75$ on a three-carbon site basis, and the reduced solubility parameter is $\tilde{\delta} = 0.61$ and thus $\delta_{PE}/\delta_{i\text{-}PP} \cong 1.51$. We quote these results not because we believe they are experimentally relevant but because they allow an unambiguous assessment of the effect of backbone stiffness on local packing and cohesive energy within the i-PP architecture.

The cohesive energy density of polymer liquids is not directly measurable and must be inferred from data using an approximate model. A recent survey by Rodgers[40] of the result of fitting six different equation-of-state theories to experimental *PVT* data has yielded cohesive energy density parameters for many polymer liquids. For "high molecular weight linear PE" (HM-LPE) and i-PP the various equation-of-state theories yield a solubility parameter ratio in the range of 1.25–1.29. For "linear polyethylene" (LPE) a value of ≅1.20 was obtained. On the other hand, additive group contribution calculations by Coleman et al.[41] yield a ratio of approximately 1.1 for a polypropylene of unspecified tacticity. In any case, the PRISM–RIS prediction seems reasonable as judged by comparison to the available experimental estimates.

PRISM–RIS calculations have also been performed for a 400 backbone carbon syndiotactic polypropylene (s-PP) melt using the Suter–Flory model at 473 K. In the syndiotactic form the RIS model predicts a significantly larger value of the characteristic ratio of 10.5. As can be seen from Figure 5, the stiffer nature of the chain and the different stereochemistry relative to i-PP result in a much shallower local correlation hole in $g(r)$. As a thermodynamic consequence, the reduced solubility parameter is found to be much larger: $\tilde{\delta} = 0.86$, which implies $\delta_{PE}/\delta_{s\text{-}PP} \cong 1.07$. Note that although s-PP has a much larger characteristic ratio than PE, the presence of methyl side groups and the attendant packing frustration "win" in the sense that s-PP still has a smaller reduced solubility parameter than the more flexible backbone polyethylene.

We are unaware of experimental *PVT* or solubility parameter data for s-PP. However, there are data on atactic polypropylene (a-PP). Since a-PP consists locally of equal fractions of the i-PP and s-PP forms (in a statistically average sense), a crude guess for the reduced solubility parameter of a-PP is a simple average of isotactic and syndiotactic values, i.e., $\tilde{\delta}_{a\text{-}PP} \cong 0.8$, which implies $\delta_{PE}/\delta_{a\text{-}PP} \cong 1.15$. This latter estimate is in reasonable agreement with the *PVT*-based experimental estimate[40] of roughly 1.11. Clearly, any definitive comparison requires an explicit PRISM–RIS treatment of a-PP.

Summarizing, our key point is that chain branching in isotactic-polypropylene reduces the effective cohesive energy density relative to polyethylene, and this can be understood in structural terms as largely due to "poorer packing", i.e., a deeper local correlation hole. The existence of deep local correlation holes in the $g(r)$'s of vinyl polymers has been unambiguously demonstrated in atomistic computer simulations of atactic-polypropylene,[45] polyisobutylene,[45] and atactic-polystyrene[46] liquids, where the chain-averaged carbon–carbon "contact value" is found to be $g(r{=}4\text{ Å}) \cong 0.2$–$0.4$.

III. Intermediate-Level Coarse-Grained Models

In this section we consider intermediate-level models which have removed some of the molecular structural detail but which are still characterized by *multiple local* chemical length scales. We have two primary goals: (1) establish how faithfully such models can reproduce various features of atomistic calculations and (2) suggest practical schemes for choosing the parameters of such intermediate-level models in an "intelligent manner", i.e., in a way that reproduces those aspects of the full problem which are deemed most important for the question of interest.

We make a simplifying approximation at the outset: the interchain interactions have the same general form as in the atomistic case, i.e., hard core site–site repulsions plus an attractive tail. For the intermediate-level models, unless stated otherwise, the attractive tail is taken to be of the Lennard-Jones-like form

$$V(r) = \epsilon\left[\left(\frac{d}{r}\right)^{12} - 2\left(\frac{d}{r}\right)^{6}\right], \quad r > d \qquad (3.1)$$

Of course, *both* the reduced liquid density (which characterizes the strength of the hard core excluded volume interactions) and the length and energy parameters of the attractive tail potential are expected to be "renormalized" from their atomistic RIS-level values. This renormalization will be implemented by "matching" certain properties of the coarse-grained and atomistic models of the polymer liquid. In particular, we require that the integrated strength of the mean field attractive energy per site, $\varrho\int d\vec{r}\ V(r)$, be independent of model. Using eqs 3.1 and 2.7 yields a relation between the reduced densities and attractive energy parameters of the two models:

$$\epsilon = \frac{8}{5}\epsilon_{LJ}\frac{\varrho_{CH_2}\sigma_{LJ}^{3}}{\varrho d^{3}} \qquad (3.2)$$

Having chosen the aspect ratio of the coarse-grained chain to match that of the RIS model, the value of reduced density ϱd^3 is set by matching the long-wavelength density fluctuations, $\hat{S}(0)$, of the atomistic and coarse-grained models of our benchmark liquid, polyethylene, at a reference temperature. We refer to this scheme of choosing the effective reduced density and attractive potential well depth for a single "reference system" as a "calibration" procedure. For other olefinic polymers (of the same chemical formula) we employ the *same* values of reduced density and attractive energy but select the aspect ratio to either reproduce the appropriate single-chain estimate or satisfy an intermolecular criterion as discussed at the end of section IIIB. Attempts to renormalize *a priori* the interaction potentials have been recently made[47,48] but are beyond the scope of the present work.

For vinyl polymers such as the polyolefins, there are two basic, but related, structural features: (a) chain branching and nonspherical monomer shape and (b) variable backbone stiffness as described by the characteristic ratio. These two features are of course not independent. The two coarse-grained models discussed here account for only one of these features explicitly. Moreover, the stereochemical aspect of tacticity cannot be described. More sophisticated, but computationally convenient, models which approximately account for both structural aspects are possible to construct and implement.

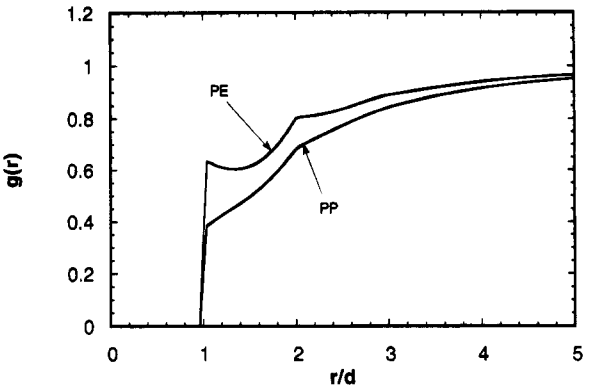

Figure 6. Chain-averaged site–site intermolecular radial distribution functions for an $N_b = 100$ freely jointed chain model of hard core "polyethylene" and "polypropylene" at a melt-like packing fraction of $\eta = 0.5$ (see ref 49).

A. Freely-Jointed Vinyl Chains. Curro[49] has recently generalized and applied the PRISM theory to treat freely-jointed, tangent hard core chains of the general vinyl architecture displayed in Figure 1. Such models have no inherent local backbone stiffness or tacticity but do account for the nonspherical monomer shape via side groups of variable hard core diameter. Here, we consider two models which are representative of PE and PP. PE is a freely-jointed linear chain of tangent sites, and PP adds a freely rotating, tangent, spherical site of identical size to every other backbone bead (see Figure 1). This model most closely represents atactic PP.

The PRISM calculations were carried out for chains composed of $N_b = 100$ backbone sites at a melt-like packing fraction of $\eta = 0.5$ in precisely the manner described in ref 49. For these conditions the value of $\hat{S}(0)$ for freely-jointed PE is close to that of the RIS PE calculation at 473 K, and this *approximately* satisfies our calibration procedure.

Results for the chain-averaged site–site $g(r)$ are shown in Figure 6. Qualitatively, the behavior is quite similar to the atomistic RIS results of Figure 5, although the difference in contact value of the PE and PP $g(r)$'s is significantly smaller for the tangent freely-jointed chain model. The reduced solubility parameters are $\delta = 0.83$ (PE) and 0.76 (PP), using the attractive potential of eq 2.7, and 0.81 (PE) and 0.71 (PP), using eq 3.1. These values should be compared with the $N_b = 400$ RIS model results of 0.92 (PE), 0.73 (i-PP), and 0.86 (s-PP). The relative solubility parameters for the two attractive potential models are $\delta_{PE}/\delta_{PP} \cong 1.09$ and 1.14, respectively, compared to the RIS model ratios of 1.26 (i-PP) and 1.07 (s-PP) and the crude RIS model estimate for a-PP of 1.15.

The freely-jointed chain results seem to be in surprisingly good agreement with the RIS–PRISM predictions for "integrated" quantities such as the cohesive energy density. The origin of this may be twofold. First, the $k = 0$ scattering of the different level models has been nearly matched. Second, the effective aspect ratios based on eq 2.13 for the freely-jointed models on a three-site basis are 1.20 for PE and 0.98 for PP versus 1.21 (PE) and 0.94 (i-PP) on a three-carbon basis, respectively, for the RIS models at 473 K. The similar behavior of the RIS and coarse-grained models suggests the most appropriate interpretation of a "site" on the freely-jointed chain may be a single carbon unit in the real polymer. Hence, under the constraint that each model displays the same value of long-wavelength

Table 1. Chain Structural Parameters at 430 K Estimated as Averages from Various Sources (Refs 10, 43, 50, 52, and 53)[a]

polymer	n_b	f_b[b]	C_∞	V_{mon} (Å^3)	Γ_{mon}	Γ_{ref}	Γ_{bond}
polyethylene (PE)	2	1	6.7	60	1.13	1.21	1.0
poly(ethylenepropylene) (PEP)	4	4/5	5.9	149	1.10	1.01	0.87
poly(vinylcyclohexane) (PVCH)	2	0.3[d]	10.6[c]	198	0.96	0.84	0.84
polypropylene (i-PP)	2	2/3	6.0	90	0.93	0.93	0.83
			4.0		0.76	0.76	0.67
polyisobutylene (PIB)	2	1/2	6.5	108	0.91	0.88	0.78
poly(ethylethylene) (PEE)	2	1/2	5.1	115	0.79	0.76	0.70
polystyrene (PS)	2	0.35[d]	10	173	0.97	0.87	
1,4-polybutadiene (PBD)	4	1	5.2	109	1.15	1.12	
1,4-polyisoprene (PI)	4	4/5	5.2	137	1.07	1.0	
1,2-polybutadiene (PVE)	2	1/2	7	110	0.95	0.91	

[a] The aspect ratios are computed from eqs 2.11 to 2.13. Two values are given for isotactic polypropylene corresponding to two different characteristic ratios. [b] Assumes all carbon units have the same volume. [c] Estimated from Table 2 of ref 52. [d] Computed assuming a volume of 60 Å^3 for the backbone part of the monomer.

density fluctuation $\hat{S}(0)$, the coarse-grained model does not necessarily represent a literal regrouping of many real carbons into a composite unit as is the usual interpretation based on a *single-chain* perspective. Rather, a "site" in the freely-jointed model might be more like an "effective carbon group" which experiences *inter*molecular interactions very similar to the (chain-averaged) real carbon units. This interpretation is consistent with our use of an interchain potential of the same basic form as appropriate for the atomistic-level model.

B. Semiflexible Chain Model. The discrete semiflexible chain (SFC) model has been discussed at length elsewhere.[11,12] The three local length scales describe chain thickness (d), effective site−site separation (bond length l) which controls the amount of site surface area available for interchain packing, and a persistence or statistical segment length which is controlled by a local bending potential of the form $-\epsilon_b(1 + \cos(\theta))$, where θ is the angle formed by three consecutive sites. Based on geometric considerations and the interpretation advanced above that a "site" in the coarse-grained chain might correspond to an effective carbon unit, the bond length should be significantly less than d in order to mimic the structure of real polymers. When combined with our $\hat{S}(0)$ calibration procedure, the results are not very sensitive to the specific choice of l/d within the structurally reasonable range of 0.4−0.6. For definitiveness, we employ a single value of $l/d = 0.5$. The density of the fluid is describable in terms of the dimensionless quantity ϱd^3.

The SFC model does not contain side groups and hence the effect of branching and tacticity enters only via an effective backbone stiffness. The simplest, and perhaps most physically appropriate, procedure based on *single-molecule* considerations is to compute an aspect ratio on an equal-volume basis using eq 2.13. Such an idea has been recently emphasized by Bates and co-workers[50] and arises naturally from thread PRISM as discussed previously[51] and in section IV. The presence of side groups results in an effectively more "flexible" or compact (smaller aspect ratio) chain. One must keep in mind that this scheme is a very crude one which neglects physical features such as side group interdigitation and/or specific packing arrangements.

Using averaged literature values[10,43,50,52,53] for the characteristic ratios, experimental densities, and a mean carbon−carbon bond length of $L = 1.5$ Å, we estimated the aspect ratios of a variety of polymers using eqs 2.11−2.13. For Γ_{ref} of eq 2.13 a reference volume of 90 Å^3 is employed which corresponds to the three-carbon repeat unit of polypropylene. For polyolefins, eq 2.11 was implemented assuming a unique value for the volume of each carbon subunit. Results for representative polyolefins and polydienes are tabulated in Table 1. Note that PE is the "stiffest" chain. Since all the polymers are flexible, their aspect ratios are roughly unity as expected on physical grounds. For a given polymer, the different definitions yield aspect ratios which may vary by 10−20%. However, the *relative* relationship between aspect ratio and polymer structure is quite insensitive to definition *within a particular class* of molecules (e.g., olefins and dienes). The values listed in the table correspond to a fixed temperature. Since polymers display widely variable thermal changes of the characteristic ratio, the relative values can change in a subtle manner with T. Alternative, possibly more useful, ways to map the real chemical structures onto a SFC with an effective stiffness based on *intermolecular* considerations are discussed below.

From Table 1 and the known value of the coil expansion coefficient for PE of $d(\ln C_\infty)/dT = -0.0011$, it is clear that the appropriate aspect ratio for PE in the common experimental temperature window falls in the range of $\Gamma_{PE} = 1.0-1.2$. In our model calculations a value of 1.2 is initially adopted. The reduced density, ϱd^3, of the SFC model of PE melt is determined by the $\hat{S}(k = 0)$ matching criterion at 430 K, i.e., $\hat{S}(0) = 0.25$ (see Figure 3). For an $N = 1000$ SFC model this leads to a value of $\varrho d^3 = 1.375$. Using eq 3.2 and the RIS-based PE potential parameters quoted in section II, one obtains for the attractive potential constant $\epsilon/\epsilon_{LJ} = 3.2$.

The corresponding hard core SFC intermolecular radial distribution function for PE is shown in Figure 7, along with the atomistic RIS result. Remarkable similarities are found, which empirically suggests a strong connection between long-wavelength density fluctuations and local interchain packing. Moreover, the reduced solubility parameter of the SFC PE model is $\tilde{\delta} = 0.87$, compared with the $N = 1000$ RIS PE value of $\tilde{\delta} = 0.89$. We do note that there is a weak decrease of $\tilde{\delta}$ with N due to a slightly deeper local correlation hole for longer chains at *fixed* density. This trend is consistent with the experimental observation of liquid densification with increasing N at fixed pressure. However, this is a finite size effect and hence the local structural and thermodynamic properties have essentially saturated when N is of order 1000 or more.

Based on eq 3.2 and the three-carbon-site estimates of effective aspect ratios of PE and i-PP (1.21 and 0.94; see Table 1), the SFC model predicts $\tilde{\delta}_{PE}/\tilde{\delta}_{PP} \cong 1.24$ for i-PP (see Figure 9). This value is in excellent agreement with the RIS model value of $\tilde{\delta}_{PE}/\tilde{\delta}_{i\text{-}PP} \cong 1.26$. For the

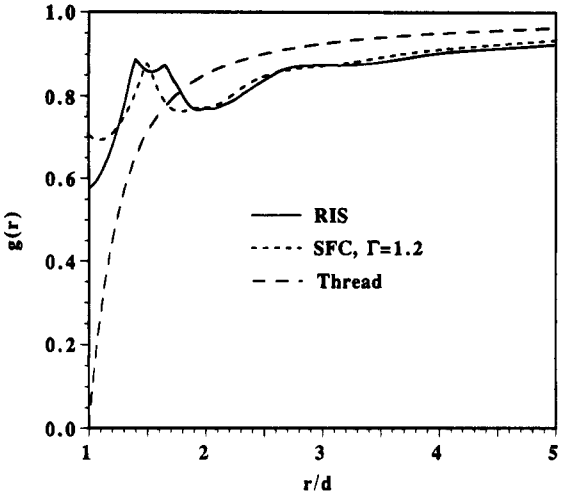

Figure 7. Interchain radial distribution function for hard core polyethylene melt at three levels: RIS model (N = 6000) at 430 K, SFC model (N = 1000), and Gaussian thread model (shifted horizontally to align the hard core diameter with the value of r/d = 1).

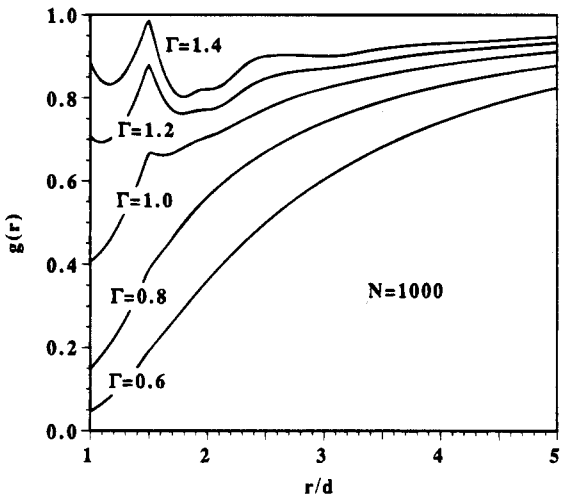

Figure 8. N = 1000, semiflexible chain model radial distribution functions for hard core melts as a function of aspect ratio.

literal Suter–Flory i-PP model corresponding to $\Gamma_{ref} \cong 0.75$, we found that $\tilde{\delta}_{PE}/\tilde{\delta}_{i\text{-}PP} \cong 1.51$, while the corresponding SFC prediction is $\tilde{\delta} \cong 0.55$ and hence $\tilde{\delta}_{PE}/\tilde{\delta}_{PP} \cong 1.58$. For the C_∞ = 10.5 s-PP RIS model, $\Gamma_{ref} \cong 1.23$ on a three-site basis, which implies at the N = 1000 SFC level $\tilde{\delta}_{PE}/\tilde{\delta}_{s\text{-}PP} \cong 1$, compared with the N = 400 RIS-level prediction of $\tilde{\delta}_{PE}/\tilde{\delta}_{i\text{-}PP} \cong 1.07$.

The results obtained above for PE and PP are encouraging, and we believe lend support to both our mapping and calibration procedures and the interpretation of a "site" in the coarse-grained model as an *effective* single-carbon unit. However, we do caution that such good agreement between the RIS and SFC model PRISM calculations may not be general. For example, as discussed below, the *a priori* single-chain mapping procedure for setting the effective aspect ratio of the SFC does not appear to be uniformly reliable in a *quantitative* sense, especially for polyolefins with side groups longer than a methyl group (e.g., PEE).

In Figure 8 a series of model calculations are presented for the $g(r)$ of SFC chain melts and a range of aspect ratios relevant to flexible polymers. In all cases a local correlation hole is found, which deepens dramatically as the chain aspect ratio is decreased. The latter corresponds to a decrease in the backbone characteristic ratio and/or more chain branching. The depth of the local hole predicted based on the mapping of Table 1 is consistent with atomistic simulations of polystyrene and polypropylene melts.[45,46]

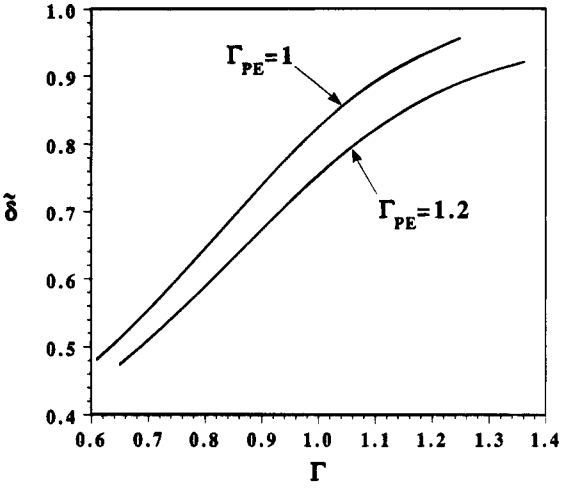

Figure 9. Reduced solubility parameter as a function of aspect ratio using the SFC melt model. The two curves correspond to two choices of the 430 K polyethylene aspect ratio coupled with the calibration procedure of choosing the melt density to reproduce the RIS PE value of $\hat{S}(0)$ at 430 K.

An important thermodynamic consequence of the structural features in Figure 8 is the sensitivity of the cohesive energy density, or reduced solubility parameter, to effective chain aspect ratio. Predictions based on eq 2.9 and 3.1 are shown in Figure 9. The two curves correspond to two choices of the aspect ratio of the reference polymer PE, where in each case the (different) reduced density was chosen to yield $\hat{S}(0)$ = 0.25. The two curves are virtually identical (i.e., superimposable) to within a multiplicative constant. When viewed as simple model calculations independent of any mapping issue, the fact that the two curves are at different reduced densities indicates the effect of pressurizing a melt to reduce its liquid volume.

The shape of the curves in Figure 9 is particularly significant. The reduced solubility parameter increases monotonically with aspect ratio as expected, and over limited regions of aspect ratio is linear. The latter feature is in agreement with recent experimental studies of Graessley et al.[7] of the solubility parameters of polyolefin liquids. However, over a broad range of aspect ratios, or under very high resolution conditions, the curve is predicted to be nonlinear: at high Γ the curve bends over while at very low aspect ratio there is upward curvature. As will be discussed elsewhere, within a regular solution approach to polymer blends these features have very important non-mean-field consequences on alloy miscibility and effective χ parameters. For example, the reduced solubility parameter difference squared, which is proportional to the χ parameter in a Hildebrand-like regular solution theory,[36] is plotted in Figure 10 for several values of the aspect ratio mismatch. The nonmonotonic nature of these curves is a consequence of the subtle nonlinearities in the solubility parameter versus aspect ratio relation.

Finally, Figure 9 suggests an alternative approach to the mapping issue. Instead of an *a priori* single-chain estimation of effective aspect ratio, one could require that it be chosen so that the relative solubility parameter in the melt agrees with the experimentally inferred value (or that deduced from computer simulation or atomistic PRISM theory). This philosophy corresponds

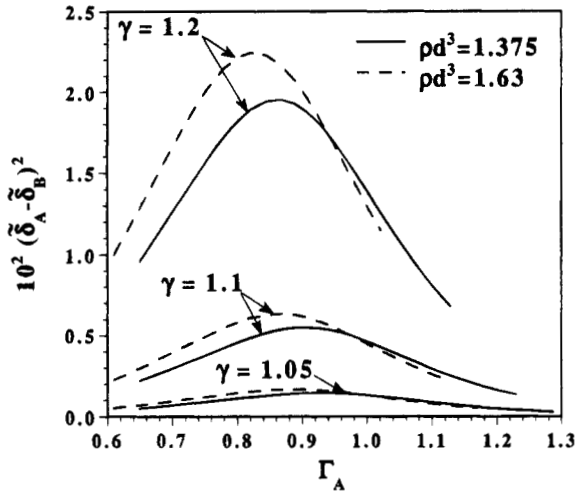

Figure 10. Square of the reduced solubility parameter difference for the SFC model as a function of aspect ratio of one polymer for various values of the stiffness asymmetry parameter $\gamma = \Gamma_B/\Gamma_A$. This quantity is proportional to the "χ-parameter" in a binary blend within regular solution theory. Results are shown for the meltlike reduced density of 1.375 and a higher density possibly relevant to a polymer liquid under pressure.

Table 2. Invariant Parameters (Å) Computed Using Information in Table 1 and Ratios of the Polyethylene Solubility Parameter to That of Various Polymers[a]

			δ_{PE}/δ		
polymer	$(\varrho_{mon}\sigma_{mon}^2)^{-1}$	δ_{PE}/δ	*PVT*	vdW	GC
PE	2.00	1	1	1	1
PEP	2.80	1.05		1.055	1.045
PIB	3.69	1.10	1.03		1.11
PP[b]	3.33, 5.0	1.08, 1.18	1.11 (a) 1.20 (i)	1.11 (a)	1.08
PEE	5.01	1.18	1.14 (i)	1.11	1.06
PVCH	4.15	1.13			0.98
PS	3.84	1.11	1.01		0.84
PBD	2.33	1.02	0.95		0.99
PI	2.93	1.06	0.98[c]		0.99
PVE	3.49	1.09			0.99

[a] Theoretical values are based on eq 4.9 and the assumption that the attractive potentials $V(r)$ are the same for all the molecules (i.e., the "bare" solubility parameter ratio associated with dispersion interaction differences is unity). The experimental estimates are from ref 40 (*PVT*; based on LPE), refs 3 and 5 (vdW), and the calculated group contribution values from ref 41 (GC). [b] The two entries for PP correspond to characteristic ratio values of 6.0 and 4.0, respectively. The symbols "a" and "i" refer to the atactic and isotactic forms. [c] Reference 6, based on modified cell model.

to a *calibration procedure for the single-chain model at the level of a bulk melt property*, which is determined by many chain interactions. Having constructed such an effective Hamiltonian of the single chain from melt information, the model plus PRISM can be employed to *predict* the behavior of polymer alloys. Although we expect that the relative ordering of aspect ratios of different chemical structures will be similar from the single-chain or melt property mapping schemes, the latter is expected to be more reliable quantitatively in alloy applications.

Typical *PVT*-inferred values of the solubility parameters according to Rodgers,[40] $\delta = (P^*)^{1/2}$, are listed in Table 2. The quoted numbers represent an average of the two most accurate equation-of-state theories: the "modified cell model"[54] and the "hole" theory of Simha and Somcynsky.[55] As an example of the alternative mapping procedure discussed above, we adopt a value of 1.2 for the PE aspect ratio and require the PRISM plus SFC model reproduce the ratio of PE to PEP and PEE melt solubility parameters suggested by Table 1, i.e., $\cong$1.05 and 1.12, respectively. Then using Figure 9 we obtain that the PEP and PEE aspect ratios must be $\cong$1.115 and 1.03, respectively. Note that although the relative ordering of the aspect ratios inferred from this mapping is the same as the single-chain-based estimates given in Table 1, these values are significantly *larger* than the single-chain Γ_{ref}. The *under*estimate of the PEE effective aspect ratio by the single-chain mapping scheme is perhaps to be expected on physical grounds since lumping side chains into an effective backbone stiffness becomes less appropriate as the side groups increase in length and experience intermolecular interdigitation. Finally, we note that if we adopt a value of 1.0 for the PE aspect ratio, then the constraint of reproducing the experimental cohesive energy density ratios yields values of 0.954 and 0.893 for the PEP and PEE aspect ratios, respectively.

IV. Analytic Gaussian Thread Model

In this section we consider the most heavily coarse-grained model: the Gaussian thread chain. Besides having the virtue of allowing analytical PRISM results to be obtained, this model may even be semirealistic in the sense that atomistic simulations show that the chain-averaged $g(r)$'s often have deep local correlation holes which approach unity in a smooth, nearly featureless manner.[45,46] Physically, this occurs not beause real molecules are Gaussian on all length scales but rather because the multitude of local chemical lengths and thermal conformational disorder conspire in a destructive manner with regards to the ensemble−averaged radial distribution function.

Within the context of PRISM theory the thread model has been discussed at length elsewhere.[12-18] Briefly, a simple Lorenztian form for the ideal random coil structure factor is adopted

$$\hat{\omega}(k) = \frac{1}{N^{-1} + (k^2\sigma^2/12)} \tag{4.1}$$

where σ is the statistical segment length and N is the number of segments. A screened Coulomb form for the attractive tail potential is employed

$$V(r) = -\epsilon\frac{\exp(-r/a)}{r/a}, \qquad \epsilon > 0 \tag{4.2}$$

where a is the spatial range and ϵ is the energy parameter. In the thread limit the hard core condition reduces to a point constraint, $g(r = 0) = 0$, and the pure hard core fluid direct correlation function assumes a δ-function form within the Percus−Yevick closure approximation, i.e., $\hat{C}(k) = \hat{C}(k = 0) = C_0$. Interaction strength in the compressible hard core fluid is characterized by the dimensionless segmental density $\varrho\sigma^3$.

In the athermal hard core limit one obtains for the site−site pair correlation function[15]

$$g_0(r) = 1 + \frac{3\sigma}{\pi\varrho\sigma^3 r}[\exp(-r/\xi_\varrho) - \exp(-r/\xi_c)] \tag{4.3}$$

where the correlation lengths are given in units of σ by

$$\xi_\varrho^{-1} = \frac{\pi}{3}\varrho\sigma^3 + \xi_c^{-1}, \qquad \xi_c = \frac{R_g}{2^{1/2}\sigma} = \left(\frac{N}{12}\right)^{1/2} \tag{4.4}$$

Note that $g_0(r)$ contains a "local" contribution from density fluctuations via the screening length ξ_ϱ and a universal "long-range correlation hole" contribution associated with the length scale ξ_c. As seen from eq 2.5, the isothermal compressibility is proportional to the $k = 0$ value of the collective structure factor which is given by[12,15]

$$\hat{S}(0) = 12\xi_\varrho^2 \propto (\varrho\sigma^3)^{-2} \quad \text{as } N \to \infty \tag{4.5}$$

Hence, the repulsive force compressibility decreases as the chain statistical segment length increases. Moreover, the thread model predicts a direct connection between the amplitude of the long-wavelength density fluctuations and the *local* correlation hole in $g(r)$. This provides theoretical support for the potential usefulness of our "calibration" procedure discussed in section III. Interesting connections between the thread PRISM predictions and prior field theoretic (two- and three-body virial coefficient formulations[56]) and blob scaling[57] approaches have also been derived.[12,15,16]

A. Cohesive Energy and Solubility Parameters. Due to its potential importance in mixing, we study the cohesive energy density and reduced solubility parameter in detail. For finite N the cohesive energy in thermal energy units is given by[58]

$$\frac{U}{U_0} = 1 - \frac{3\sigma}{\pi a}(\varrho\sigma^3)^{-1}\left[\frac{1}{1+(a/\xi_c)} - \frac{1}{1+(a/\xi_\varrho)}\right]$$
$$= \frac{a}{a+\xi_\varrho} = \frac{1}{1+\dfrac{3}{\pi\varrho\sigma^2 a}}, \quad \text{as } N \to \infty \tag{4.6}$$

where $U_0 = -2\pi\beta\epsilon\varrho^2a^3$ is the corresponding "mean field" value appropriate to the limit $g(r) = 1$. Examination of the first form above shows that the solubility parameter decreases weakly with N (finite size effect) due to the interference between the local density screening and the long-range correlation hole length scales and the enhanced self-shielding effect.[13] Some experimental evidence for this trend exists for polystyrene[59] and poly(ethylenepropylene) (PEP)[60] oligomer melts.

In the long-chain limit ($\xi_\varrho/\xi_c \to 0$) one obtians a very simple expression for the reduced solubility parameter:

$$\tilde{\delta} = \frac{1}{\left(1+\dfrac{3}{\pi\varrho\sigma^2 a}\right)^{1/2}} = \frac{1}{\left(1+\xi_\varrho\dfrac{\sigma}{a}\right)^{1/2}} \tag{4.7}$$

The relevant dimensionless density involves all three local nonuniversal length scales: the density screening length, the attractive potential range, and the chain statistical segment length. For a fixed attractive potential range, this relation predicts that for thread melts the only relevant quantity is the statistical segment length squared per unit volume, $\varrho\sigma^2$. Such a result was previously obtained for athermal conformationally asymmetric thread blends by Curro and Schweizer.[51] The importance of such an invariant quantity in blends of conformationally asymmetric polymers has been recently emphasized by Bates and co-workers[50] in the context of quasi-universal unfavorable excess entropy of mixing.[61] Here, we see that this invariant quantity, the "segment length on an equal-volume basis", arises rigorously from the melt PRISM theory for the enthalpy-based solubility parameter of thread chains.

The reduced solubility parameter is predicted to increase as the chain stiffness on an equal-volume basis increases. Equation 4.7 also predicts that as the attractive potential becomes spatially longer ranged the reduced solubility parameter will increase since the shallower region of the local correlation hole is sampled more heavily (i.e., $g(r) = 1$ is a better approximation). Finally, note that in the hypothetical incompressible limit ($\varrho \to \infty$) the reduced solubility parameter is unity, independent of system parameters since $g(r) = 1$ becomes exact.

It is instructive to rewrite eq 4.7 in two additional forms. Defining the melt packing fraction as $\eta = \pi\varrho d^3/6$ and the aspect ratio as $\Gamma = \sigma/d$ and using eqs 4.4 and 4.5 yield

$$\tilde{\delta} = \frac{1}{\left(1+\dfrac{d/a}{2\eta\Gamma^2}\right)^{1/2}} = \frac{1}{\left(1+\dfrac{\sigma}{a}\left(\dfrac{\hat{S}(0)}{12}\right)^{1/2}\right)^{1/2}} \tag{4.8}$$

In these forms it is clear that the reduced solubility parameter is predicted to decrease as the liquid becomes more compressible (see eq 2.5) or the aspect ratio decreases. This qualitative prediction is very general; i.e., it holds for all level of models studied (RIS, FJC, SFC, thread). Such structure–property correlations are *globally* supported by the recent small-angle neutron scattering (SANS) and *PVT* measurements on polyolefins by Graessley et al.[3,5,7]

B. Mappings and Comparison with Experiments. The question of how to map a real polymer structure *onto the thread model* seems to have a unique answer: only the segment length on an equal-volume basis is relevant. Given a value for the attractive potential range, a, eq 4.7 or 4.8 can be used to calculate the reduced solubility parameters of polymer melts. For Lennard-Jones-like interactions, $a/d = 0.5$ is a reasonable estimate.[15] Following our mapping and calibration procedures, for PE at 430 K one has $\hat{S}(0) = 0.25$ and $\sigma/d = 1.2$, which when substitued into the second form of eq 4.8 yield $\delta = 0.86$. This value is in surprisingly good (perhaps fortuitous) agreement with the $N = 1000$ RIS PE value of $\tilde{\delta} = 0.87$ and $\tilde{\delta} = 0.89$ for the SFC model.

The predicted thread pair correlation function is plotted in Figure 7 and is seen to represent a reasonable "interpolation" of both the RIS and the SFC model predictions. This behavior is presumably the reason that an integrated quantity such as the reduced cohesive energy seems rather insensitive for PE to the level of chemical structure retained. The key feature appears to be a correct calibration of the $k = 0$ density fluctuations (i.e., $\hat{S}(0)$), which then places significant constraints on the local correlation hole region of $g(r)$.

The general prediction of the thread model for the reduced solubility parameter based on two choices of the PE thread aspect ratio (but with the common calibration procedure) and the first form of eq 4.8 is shown in Figure 11. The two thread curves are virtually identical to within a multiplicative constant. However, the dependence of the reduced solubility parameter on aspect ratio is much gentler in the thread model compared with the less-coarse-grained SFC model. Perhaps this is to be expected given the complete absence of local chain rigidity and sharp structural packing features in the thread model. The *quantitative* differences between the thread and SFC curves emphasize the potential importance of choosing the aspect ratios of a given polymer via the melt property mapping scheme, not the *a priori* single-chain mapping procedure.

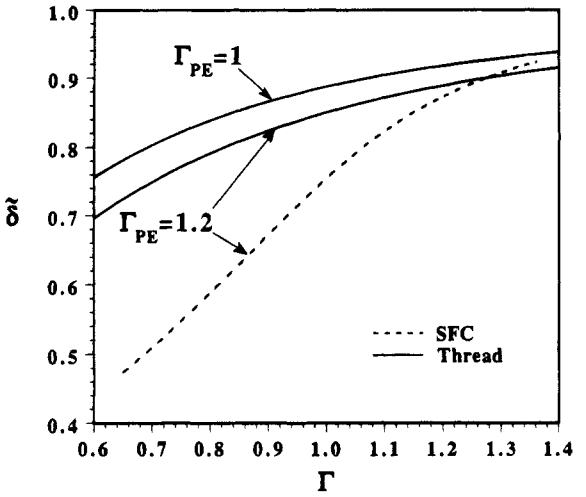

Figure 11. Reduced solubility parameter as a function of aspect ratio for the SFC model and analytic Gaussian thread model. Two choices of the polyethylene aspect ratio at 430 K are shown with the density determined by the calibration procedure discussed in the text.

It is interesting to explore what the thread model generally predicts according to the *a priori* single-chain mapping scheme. We employ eq 4.7 with the invariant quantity $\varrho\sigma^2 = \sigma_{mon}^2/V_{mon}$ computed (in units of inverse angstroms) as described in section II with the data of Table 1. The value of a is chosen so the result obtained above for PE, $\delta = 0.86$, is maintained. This constraint implies

$$\tilde{\delta} = \frac{1}{\left(1 + \frac{0.176}{\varrho_{mon}\sigma_{mon}^2}\right)^{1/2}} \tag{4.9}$$

The calculated solubility parameters relative to the PE value are listed in Table 2. Also listed are the average values inferred by Rodgers[40] based on the most accurate MCM[54] and cell model[55] *PVT* equations-of-state. These numbers use the "linear polyethylene" data as the reference state. For comparison, also listed are selected polyolefin values as obtained by Graessley et al.[3,5,7] assuming a van der Waals liquid model: $\delta \cong T(\alpha/\kappa_T)^{1/2}$, where κ_T is the measured isothermal compressibility and α is thermal expansion coefficient. Calculated estimates based on the molar attraction constants and group additivity scheme[41] are also shown. We note that these latter calculations treat methyne, methylene, and methyl groups as energetically distinct. However, our theoretical estimates are based on eq 2.9 with the simplifying assumption that the effective bare dispersion energies in all the polyolefins with the same chemical formula are the same. Thus, our theoretical results in Table 2 refer only to the "structural/local packing" aspect of the solubility parameter. This perhaps explains why our numbers are consistently too high for the unsaturated molecules (PS and polydienes), which are expected to experience stronger dispersive interactions associated with the presence of more polarizable carbon double bond(s). If the "bare" chemical interaction differences can be estimated, then our results can be corrected in a trivial multiplicative manner.

Several additional points concerning Table 2 warrant comment. (1) For many of the olefins the group contribution estimate is smaller than the *PVT*-derived values. This has been pointed out by several recent workers.[3-5,7,50] It perhaps is indicative that the bond additivity scheme emphasizes primarily the "bare" chemical differences and misses the structural/packing part of the problem. (2) The predicted near equivalence of the solubility parameters of saturated PE and unsaturated PBD and PVE is surprising since they differ in both bare chemical interactions and effective aspect ratio. Perhaps this is an exmaple of the chemical and structural asymmetries tending to "compensate" for each other as discussed previously.[18] (3) The group additivity scheme predicts poly(vinylcyclohexane) (PVCH) has a higher solubility parameter than PE. Based on effective aspect ratio/packing consideration, just the opposite would be expected. Extraction of the cohesive energy density of PVCH from experimental *PVT* measurements would an interesting test of the effective aspect ratio ideas.

The overall reasonable agreement between our *a priori* theoretical estimates of the relative solubility parameter for the polyolefins and the experimentally derived values is intriguing. It might imply the simplest, single-molecule approach to estimating the appropriate chain stiffness is accurate when employed within the thread framework. Alternatively, such agreement may be fortuitous, and the melt calibration procedure is perhaps the most reliable procedure. A definitive conclusion cannot be given at present, and more research is required in order to develop an empirical feeling for the general reliability of the Gaussian thread and stiffness on equal-volume approaches.

Finally, we emphasize that the estimates in Table 2 depend on temperature and pressure (density) through both the melt density and effective segment length. Thus, the concept of a single solubility parameter for a specific polymer, which is implicit to both the *PVT*-based approaches and molar attraction constant estimates, is not really adequate. This conclusion is consistent with regular solution theory arguments[36] and recent experiments.[5,7]

V. Summary and Discussion

In this work we have explored as a function of level of chemical structural detail the interchain packing, cohesive energy, and solubility parameters of polymer melts with a primary focus on polyolefins. From the chemically realistic RIS-level calculations on polyethylene and polypropylene, we found that chain branching strongly enhances the local correlation hole in the interchain radial distribution function, which results in a smaller solubility parameter. Comparisons of these atomistic-level calculations with available experimental and simulation data[2,21,45,46] are encouraging. We then explored the structural and solubility parameter predictions of more coarse-grained models based on a density fluctuation based calibration procedure and a single-chain mapping scheme. Some support for the idea that chain branching can be mimicked by an effective aspect ratio for purposes of calculating a chain-averaged $g(r)$ and cohesive energy density was found, in qualitative accord with very recent simulations of coarse-grained, branched polymer fluids.[62] Using the SFC model for the "chemically symmetric" case, a globally nonlinear correlation between reduced solubility parameter and effective aspect ratio was found. A one-to-one correspondence between the solubility parameter and effective segment length within a homologous series of hydrocarbon polymers appears to be supported (at least in a global sense) by recent polyolefin SANS and *PVT*

experiments.[3-5,7] Surprisingly, the analytic Gaussian thread model also appears reasonable, especially for an "integrated" quantity such as the solubility parameter. A many-chain, melt-property-based mapping scheme was also advanced and suggested to be more quantitatively accurate for polymer alloy applications.

All our analysis has employed the van der Waals idea that the interchain pair correlations in dense liquids are determined entirely by the repulsive (modeled as hard core) branch of the potential. For more subtle questions such as the temperature dependence of solubility parameters, corrections associated with the influence of the attractive forces on local packing may be nonnegligible. We have also only coarse-grained the polymer structure, not the form of the intermolecular potentials. A more sophisticated approach would consider this latter aspect also.

Despite the successes of the coarse-grianed models, they must have limitations. Such models cannot describe specific packing arrangements as may arise in certain melts or blends of branched polymers. Moreover, if the monomer is chemically inhomogeneous (i.e., not just methylene-like groups), then the reduction of a many inequivalent site representation of monomer structure to the SFC or Gaussian thread levels will probably be less reliable and may fail entirely in some cases (e.g., specific interaction). More melt studies of the connections between the atomistic-level predictions of PRISM and those obtained from coarse-grained models are planned in order to shed additional light on these subtle issues.

We expect the simpler coarse-grained models will be of most use within a homologous series of polymers, e.g., the polyolefins or polydienes. For such systems the bare chemical interactions are of the simple dispersion form and relatively constant as a function of chain microstructure. Moreover, it may be that a homologous series of random copolymers will conform best to the simple models (e.g., ethylene/1-butene[3-5,7] or ethylene/propylene[6]). Physically, this may be true since the quenched sequence disorder and attendant irregular effective chain thickness of such polymers will tend to inhibit specific packing arrangements and provide a more uniform chain contour profile in a statistically averaged sense. These features may thus serve to make a single site effective homopolymer description such as the SFC or Gaussian thread model more accurate in a "self-averaging" sense.

One may ask why bother with these coarse-grained models if atomistic-level PRISM calculations are now feasible? There are several answers. (1) For many polymers of interest RIS or atomistic models and/or intermolecular potentials are either nonexistent or inaccurate. (2) The required RIS single-chain structure factors must be computed from a molecular dynamics or Monte Carlo simulation which may be tedious if one is interested in a wide range of temperatures and the determination of phase boundaries. (3) The development of a general understanding of trends and relative behavior of a wide class of polymer alloys may be greatly facilitated, from both computational and conceptual points of view, by use of "intelligently constructed" coarse-grained models. Moreover, it is an interesting and important problem to learn when coarse-grained models work and when they fail, i.e., how much chemical detail is required to understand a particular physical question. A definitive answer to this question requires more research, but theoretical results for atomistic models will certainly be invaluable. Single-chain simulations based on available rotational and interatomic potentials are now quite feasible for modest chain lengths. Generalization to long chain can be done in a computationally convenient and accurate manner as discussed, for example, in ref 37. Numerical solution of the many coupled nonlinear PRISM integral equations for atomistic multisite models based on the Picard iteration scheme also does not seem to be a significant difficulty.[63] Thus, chemically realistic multisite PRISM calculations for a broad class of polymer melts and blneds are also now possible and beginning to be widely implemented.[63] The choice of atomistic versus coarse-grained models is a subtle one which will depend on the problem and system of interest, the desired accuracy of the theoretical predictions, and the level of computational convenience deemed acceptable.

Finally, a primary motivation for our present melt work is its potential use to study polymer alloys and the connection between microscopic structure and miscibility. Any general insights that can be gleaned from studying the computationally convenient coarse-grained models would be extremely valuable from a molecular design and engineering point of view. The simplest application of the present work to polymer blends is to adopt regular solution theory to estimate mixing behavior and effective χ parameters directly from knowledge of computed melt properties (e.g., see Figure 10). The reliability of such a scheme is presently under study, and detailed applications to polyolefin alloys will be reported elsewhere.[64]

Acknowledgment. Many helpful and stimulating discussions with W. W. Graessley and R. Krishnamoorti are gratefully acknowledged. Work at Illinois was supported by the Division of Materials Sciences, Office of Basic Energy Sciences, U.S. Department of Energy, in cooperation with Oak Ridge National Laboratory and the UIUC Materials Research Laboratory (via Grant No. DEFG02-91ER45439). Support from the central computing facilities of the UIUC–MRL is also gratefully acknowledged. At Sandia National Laboratories and the University of New Mexico, funding came from the U.S. Department of Energy under Contract DE-AC047DP00789 and also the Basic Energy Sciences/ Division of the Materials Research Program.

References and Notes

(1) Schweizer, K. S.; Curro, J. G. *Phys. Rev. Lett.* **1987**, *58*, 246. Curro, J. G.; Schweizer, K. S. *Macromolecules* **1987**, *20*, 1928.
(2) For a recent review, see: Schweizer, K. S.; Curro, J. G. *Adv. Polym. Sci.* **1994**, *116*, 319.
(3) Graessley, W. W.; Krishnamoorti, R.; Balsara, N. P.; Butera, R. J.; Fetters, L. J.; Lohse, D. J.; Schulz, D. N.; Sissano, J. A. *Macromolecules* **1994**, *27*, 3896.
(4) Graessley, W. W.; Krishnamoorti, R.; Balsara, N. P.; Fetters, L.J.; Lohse, D. J.; Schulz, D. N.; Sissano, J. A. *Macromolecules* **1994**, *27*, 2574.
(5) Krishnamoorti, R.; Graessley, W. W.; Balsara, N. P.; Lohse, D. J. *Macromolecules* **1994**, *27*, 3073.
(6) Walsh, D. J.; Graessley, W. W.; Datta, S.; Lohse, D. J.; Fetters, L. J. *Macromolecules* **1992**, *25*, 5236.
(7) Graessley, W. W.; Krishnamoorti, R.; Reichart, G. C.; Balsara, N. P.; Fetters, L. J.; Lohse, D. J., preprint, 1994.
(8) Sanchez, I. C. *Annu. Rev. Mater. Sci.* **1983**, *13*, 387.
(9) Paul, D. R.; Barlow, J. W. In *Polymer Compatibility and Incompatibility*; Sole, K., Ed. MMI: Midland, MI, 1981; p 1. Sanchez, I. C. *Ibid*, p 59.
(10) Flory, P. J. *Statistical Mechanics of Chain Molecules*; Hanser: Munich, 1969.
(11) Honnell, K. G.; Curro, J. G.; Schweizer, K. S. *Macromolecules* **1990**, *23*, 3496.

(12) Schweizer, K. S.; Honnell, K. G.; Curro, J. G. *J. Chem. Phys.* **1992**, *96*, 3211.
(13) Schweizer, K. S.; Curro, J. G. *Macromolecules* **1988**, *21*, 3070, 3082.
(14) Schweizer, K. S.; Curro, J. G. *J. Chem. Phys.* **1991**, *94*, 3986.
(15) Schweizer, K. S.; Curro, J. G. *Chem. Phys.* **1990**, *149*, 105.
(16) Melenkevitz, J.; Curro, J. G.; Schweizer, K. S. *J. Chem. Phys.* **1993**, *99*, 5571.
(17) Schweizer, K. S. *Macromolecules* **1993**, *26*, 6033.
(18) Schweizer, K. S. *Macromolecules* **1993**, *26*, 6050.
(19) Honnell, K. G.; McCoy, J. D.; Curro, J. G.; Schweizer, K. S.; Narten, A. H.; Habenshuss, A. *J. Chem. Phys.* **1991**, *94*, 4659.
(20) Narten, A. H.; Habenshuss, A.; Honnell, K. G.; McCoy, J. D.; Curro, J. G.; Schweizer, K. S. *J. Chem. Soc., Faraday Trans.* **1992**, *13*, 1791.
(21) Dodd, L. R.; Theodorou, D. N. *Adv. Polym. Sci.* **1994**, *116*, 249.
(22) Yethiraj, A.; Curro, J. G.; Schweizer, K. S.; McCoy, J. D. *J. Chem. Phys.* **1993**, *98*, 1635.
(23) Curro, J. G.; Yethiraj, A.; Schweizer, K. S.; McCoy, J. D.; Honnell, K. G. *Macromolecules* **1993**, *26*, 2655.
(24) Sen, S.; Cohen, J.; McCoy, J. D.; Curro, J. G. *J. Chem. Phys.* **1994**, *101*, 9010.
(25) Woodward, C. E.; Yethiraj, A. *J. Chem. Phys.* **1994**, *100*, 3181. Yethiraj, A.; Woodward, C. E. *J. Chem. Phys.*, submitted.
(26) Yethiraj, A.; Hall, C. K. *J. Chem. Phys.* **1991**, *95*, 3749.
(27) Walley, K. P.; Schweizer, K. S.; Peanasky, J.; Cai, L.; Granck, S. *J. Chem. Phys.* **1994**, *100*, 3361.
(28) McCoy, J. D.; Honnell, K. G.; Schweizer, K. S.; Curro, J. G. *J. Chem. Phys.* **1991**, *95*, 9348.
(29) See, for example: *Atomistic Modeling of Physical Properties*; *Advances in Polymer Science*; Monnerie, L., Suter, U. W., Eds.; Springer-Verlag: Berlin, 1994.
(30) Andersen, H. C.; Chandler, D.; Weeks, J. D. *Adv. Chem. Phys.* **1976**, *34*, 105.
(31) Hansen, J. P.; McDonald, I. R. *Theory of Simple Liquids*, 2nd ed.; Academic Press: London, 1986.
(32) Chandler, D. In *Studies in Statistical Mechanics VIII*; Montroll, E., Lebowitz, J., Eds.; North-Holland: Amsterdam, 1982; p 274.
(33) Barker, J. A.; Henderson, D. *Annu. Rev. Phys. Chem.* **1972**, *23*, 439.
(34) Chandler, D. *Chem. Phys. Lett.* **1987**, *139*. 108.
(35) Curro, J. G.; Schweizer, K. S. *J. Chem. Phys.* **1987**, *87*, 184.
(36) Rowlinson, J. S.; Swinton, F. L. *Liquids and Liquid Mixtures*; Butterworth Scientific: London, 1982. Hildebrand, J.; Scott, R. *The Solubility of Nonelectrolytes*, 3rd ed.; Reinhold: New York, 1949.
(37) McCoy, J. D.; Honnell, K. G.; Curro, J. G.; Schweizer, K. S.; Honeycutt, J. D. *Macromolecules* **1992**, *25*, 4905.
(38) Zoller, P. *J. Appl. Polym. Sci.* **1979**, *23*, 1051; *J. Polym. Sci., Polym. Phys. Ed.* **1980**, *18*, 897.
(39) McCoy, J. D., private communication. Nath, S. K.; McCoy, J. D.; Curro, J. G. *J. Chem. Phys.*, to be published.
(40) Rodgers, P. A. *J. Appl. Polym. Sci.* **1993**, *48*, 1061.
(41) Coleman, M. M.; Serman, C. J.; Bhagwagar, D. E.; Painter, P. *Polymer* **1990**, *31*, 1187.
(42) Suter, U. W.; Flory, P. J. *Macromolecules* **1975**, *8*, 765.
(43) Zirkel, A.; Urban, V.; Richter, D.; Fetters, L. J.; Huang, J. S.; Kampmann, R.; Hadjichristidis, N. *Macromolecules* **1992**, *25*, 6148.
(44) Curro, J. G.; Rajasekaran, J. J., in preparation.
(45) Theodorou, D. N.; Suter, U. W. *Macromolecules* **1985**, *18*, 1467. Han, J.; Boyd, R. *Macromolecules* **1994**, *27*, 5365.
(46) Khare, R.; Paulaitis, M. E.; Lustig, S. R. *Macromolecules* **1993**, *26*, 7203.
(47) Rodriguez, A. L.; Freire, J. J. *Mol. Phys.* **1988**, *63*, 591; **1991**, *73*, 691.
(48) Lee, K.; Adams, J. B.; Schweizer, K. S., in preparation.
(49) Curro, J. G. *Macromolecules* **1994**, *27*, 4665.
(50) Bates, F. S.; Schulz, M. F.; Rosedale, J. H. *Macromolecules* **1992**, *25*, 5547. Bates, F. S.; Fredrickson, G. F. *Macromolecules* **1994**, *27*, 1065.
(51) Curro, J. G.; Schweizer, K. S. *Macromolecules* **1990**, *23*, 1402.
(52) Gehlsen, M. D.; Bates, F. S. *Macromolecules* **1994**, *27*, 3611.
(53) Zirkel, A.; Richter, D.; Pyckhout-Hintzen, W.; Fetters. L. J. *Macromolecules* **1992**, *25*, 954. Mays, J.; Hadjichristidis, N.; Fetters, L. J. *Macromolecules* **1984**, *17*, 2723.
(54) Dee, G. T.; Walsh, D. J. *Macromolecules* **1988**, *21*, 811, 815.
(55) Simha, R.; Somcynsky, T. *Macromolecules* **1969**, *2*, 342.
(56) Doi, M.; Edwards, S. F. *The Theory of Polymer Dynamics*; Clarendon Press: Oxford, 1986. Muthukumar, M. *J. Chem. Phys.* **1986**, *85*, 4722.
(57) de Gennes, P.-G. *Scaling Concepts in Polymer Physics*; Cornell University Press: Ithaca, NY, 1979.
(58) Schweizer, K. S.; Yethiraj, A. *J. Chem. Phys.* **1993**, *98*, 9053.
(59) Ougizawa, T.; Dee, G. T.; Walsh, D. J. *Polymer* **1989**, *30*, 1675.
(60) Chen, S.-J.; Chiew, Y. C.; Garddecki, J. A.; Nilsen, S.; Radosz, M. *J. Polym. Sci., B: Polym. Phys.* **1994**, *32*, 1791.
(61) Fredrickson, G. H.; Liu, A. J.; Bates, F. S. *Macromolecules* **1994**, *27*, 2503.
(62) Yethiraj, A.; Curro, J. G.; Rajasekaran, J. J. *J. Chem. Phys.*, submitted. Kacker, N.; Kumar, S. K. *Polym. Prep. (Am. Chem. Soc., Div. Polym. Chem.)*, to be published.
(63) Rajasekaran, J. J.; Curro, J. G. *Macromolecules*, to be submitted.
(64) Schweizer, K. S.; Singh, C. *Macromolecules*, in press.

MA941262M